Cell Reports

Report

Extracellular Acidosis and mTOR Inhibition Drive the Differentiation of Human Monocyte-Derived Dendritic Cells

Graphical Abstract

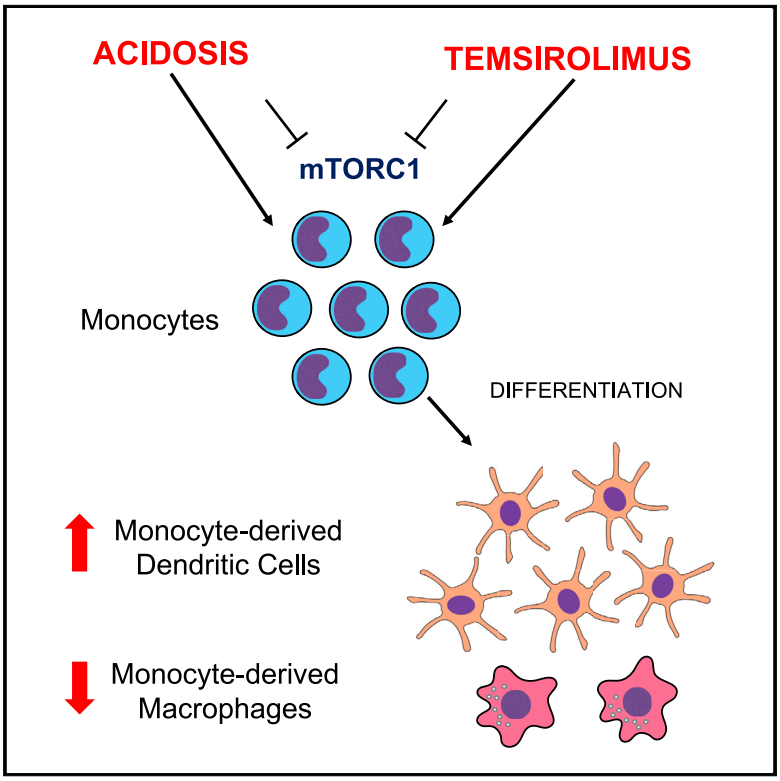

Authors

Fernando Erra Díaz, Valeria Ochoa, Antonela Merlotti, ..., Sebastián Amigorena, Elodie Segura, Jorge Geffner

Correspondence

jorgegeffner@gmail.com

In Brief

Erra Díaz et al. show that low pH, a hallmark of inflammation and the tumor microenvironment, markedly promotes the differentiation of human monocytes into dendritic cells through a process associated with the inhibition of mTORC1. Moreover, the authors describe that pharmacological mTORC1 inhibition at neutral pH also promotes dendritic cell differentiation.

Highlights

- Low pH promotes monocyte differentiation into dendritic cells (mo-DCs)
- Low pH inhibits mTORC1 activity
- mTORC1 inhibition promotes mo-DC differentiation at neutral pH
- mTORC1 inhibition turns GM-CSF into a strong inducer of mo-DC differentiation

Erra Díaz et al., 2020, Cell Reports *31*, 107613
May 5, 2020
https://doi.org/10.1016/j.celrep.2020.107613

CellPress

Cell Reports

CellPress
OPEN ACCESS

Report

Extracellular Acidosis and mTOR Inhibition Drive the Differentiation of Human Monocyte-Derived Dendritic Cells

Fernando Erra Díaz,[1] Valeria Ochoa,[1] Antonela Merlotti,[2] Ezequiel Dantas,[1] Ignacio Mazzitelli,[1] Virginia Gonzalez Polo,[1] Juan Sabatté,[1] Sebastián Amigorena,[2] Elodie Segura,[2] and Jorge Geffner[1,3,*]

[1]INBIRS, Universidad de Buenos Aires (UBA)-CONICET, Buenos Aires, Argentina
[2]Institut Curie, PSL Research University, INSERM, U932 Paris, France
[3]Lead Contact
*Correspondence: jorgegeffner@gmail.com
https://doi.org/10.1016/j.celrep.2020.107613

SUMMARY

During inflammation, recruited monocytes can differentiate either into macrophages or dendritic cells (DCs); however, little is known about the environmental factors that determine this cell fate decision. Low extracellular pH is a hallmark of a variety of inflammatory processes and solid tumors. Here, we report that low pH dramatically promotes the differentiation of monocytes into DCs (monocyte-derived DCs [mo-DCs]). This process is associated with a reduction in glucose consumption and lactate production, the upregulation of mitochondrial respiratory chain genes, and the inhibition of mTORC1 activity. Interestingly, we also find that both serum starvation and pharmacological inhibition of mTORC1 markedly promote the differentiation of mo-DCs. Our study contributes to better understanding the mechanisms that govern the differentiation of monocytes into DCs and reveals the role of both extracellular pH and mTORC1 as master regulators of monocyte cell fate.

INTRODUCTION

Dendritic cells (DCs) play a critical role in the initiation of the adaptive immune response and the maintenance of self-tolerance (Banchereau and Steinman, 1998; Hawiger et al., 2001). Three major subsets of DCs have been defined in the steady state: plasmacytoid DCs (pDCs), type 1 conventional DCs (cDC1), and type 2 cDCs (Geissmann et al., 2010; Guilliams et al., 2014; Merad et al., 2013; Mildner and Jung, 2014). Inflammatory processes are associated with the development of an additional DC subset, so-called monocyte-derived DCs (mo-DCs) (Boltjes and van Wijk, 2014; Cheong et al., 2010; Greter et al., 2012; Segura and Amigorena, 2013; Shortman and Naik, 2007). mo-DCs have also been described in steady-state conditions (Richter et al., 2018; Tamoutounour et al., 2013; Coillard and Segura, 2019).

Low pH is a hallmark of a variety of inflammatory processes in peripheral tissues. Values of extracellular pH as low as 6.0 have been described in the course of inflammation triggered by bacterial infections (Abbot et al., 1990; Bryant et al., 1980; Dubos, 1955; Edlow and Sheldon, 1971; Simmen et al., 1994; Simmen and Blaser, 1993) and also in the context of autoimmune diseases (Geborek et al., 1989; Månsson et al., 1990). Moreover, extracellular acidosis (range, 5.8 to 7.4) is a hallmark of solid tumors as well as a major determinant of tumor progression (Ashby, 1966; Corbet and Feron, 2017; Helmlinger et al., 1997).

Little is known about the factors that determine whether monocytes will differentiate into macrophages or DCs. Using human monocytes, we report here that low pH and mTORC1 inhibition markedly promote the differentiation of mo-DCs.

RESULTS

Low pH Skews the Differentiation of Monocytes into DCs

Goudot et al. (2017) have shown that culturing monocytes with macrophage colony stimulating factor (M-CSF), interleukin-4 (IL-4), and tumor necrosis factor alpha (TNF-α) yields a heterogeneous population of cells, including a subpopulation of mo-DCs ($CD1a^+CD16^-$ cells). Using this approach, we analyzed the influence exerted by extracellular pH on the differentiation of mo-DCs. Figure 1A shows that pH 6.5 markedly promoted the differentiation of monocytes into DCs ($CD1a^+CD16^-$ cells). Quantification of the absolute number of cells in each cell population (Figure 1A, right panel) and kinetic studies (Figure S1A) confirmed that the enrichment in $CD1a^+CD16^-$ cells at pH 6.5 reflected an enhanced differentiation of monocytes into DCs and not a reduction in the viability of $CD1a^-$ cells. Even a small reduction in the pH resulted in an enhanced frequency of mo-DCs. In fact, a significant increase in DC differentiation was observed at pH 7.0 compared with pH 7.3 ($p < 0.01$, $n = 5$) (Figure 1B). At pH values lower than 6.0, a progressive decline in cell viability was observed after 2 days of culture (data not shown), precluding the analysis of DC differentiation. Interestingly, the culture of monocytes at pH 6.5 for 24 h followed by an additional period of 4 days at pH 7.3 significantly promoted the differentiation of DCs, whereas the culture of monocytes at pH 6.5 for 3 days,

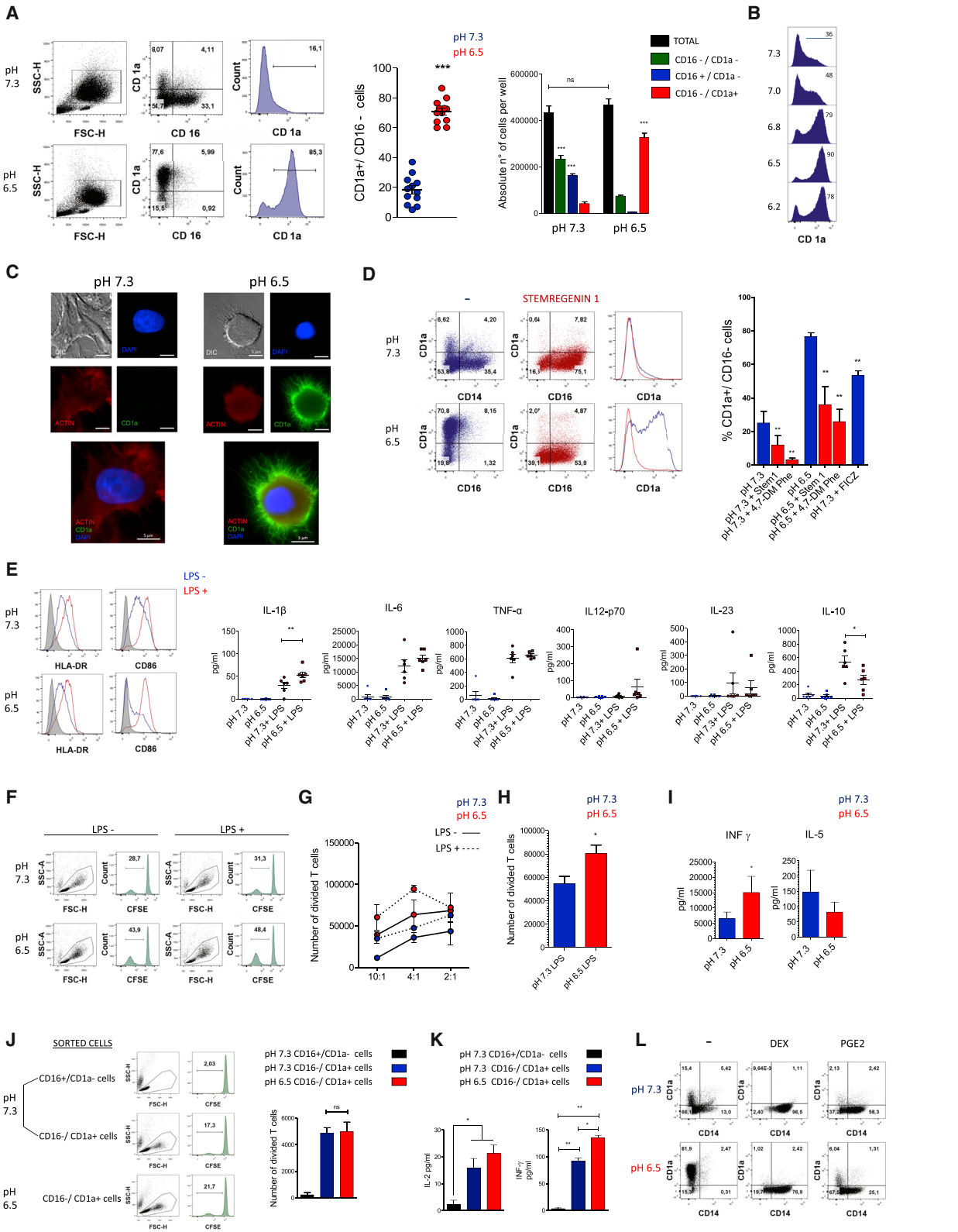

(legend on next page)

followed by 2 days at pH 7.3, promoted DC differentiation in a similar fashion as monocytes cultured for 5 days at pH 6.5 (Figure S1B). Further studies were performed to determine whether acidosis might bypass the requirement of M-CSF, IL-4, or TNF-α for mo-DC differentiation. In the absence of M-CSF, high apoptosis levels were observed early in the cultures, either at pH 7.3 or pH 6.5 (data not shown). Acidosis was shown to be unable to induce the differentiation of mo-DCs in the absence of IL-4 but significantly promoted their differentiation in the absence of TNF-α (Figure S1C).

Morphological studies revealed that most of the cells cultured with M-CSF, IL-4, and TNF-α at pH 6.5 showed a typical DC morphology, whereas cells cultured at pH 7.3 differentiated into macrophage-like cells (Figure 1C). Differentiation of mo-DCs has been shown to be dependent on the activity of the aryl hydrocarbon receptor (AHR) (Goudot et al., 2017). Using two AHR inhibitors, stemregenin-1 or 4,7-dimethyl-1,10-phenanthroline (4,7-DM Phe), we found a marked prevention of mo-DCs differentiation at low pH. In contrast, the natural AHR agonist 6-formylin-dolo (3,2-b) carbazole (FICZ) significantly promoted DC differentiation at pH 7.3 (Figure 1D). These results suggest that AHR plays an important role in the differentiation of mo-DCs.

Functional studies revealed an increased expression of human leukocyte antigen (HLA)-DR and CD86 upon lipopolysaccharide (LPS) stimulation in cultures performed at pH 7.3 or pH 6.5 (Figure 1E, left panel). Cells cultured at pH 6.5 showed a higher production of IL-1β and a lower production of IL-10 upon LPS stimulation (Figure 1E, right panel). Moreover, they showed a high ability to induce the proliferation of allogeneic T cells (Figures 1F–1H) and the production of IFN-γ by alloreactive lymphocytes (Figure 1I). To better characterize the functional profile of mo-DCs we also used sorted cells. Sorted $CD16^-$ $CD1a^+$ cells (mo-DCs) obtained at either pH 7.3 or 6.5 produced higher levels of IL-1β and lower levels of IL-10 upon LPS stimulation than $CD16^+$ $CD1a^-$ cells ($n = 4$, $p < 0.01$). As expected, sorted $CD16^+$ $CD1a^-$ cells displayed a negligible ability to induce the proliferation and the production of IL-2 and IFN-γ by allogeneic T cells. In contrast, $CD16^-$ $CD1a^+$ cells (mo-DCs) obtained at either pH 7.3 or 6.5 showed a high ability to induce both responses (Figures 1J and 1K). Consistent with the ability of corticosteroids and prostaglandin E2 (PGE2) to promote the development of tolerogenic DCs (Kaliński et al., 1997; Obermajer et al., 2011; Woltman et al., 2000), we found that dexamethasone and PGE2 almost completely prevented the differentiation of mo-DCs either at pH 7.3 or pH 6.5 (Figure 1L).

Having shown the ability of low pH to promote the differentiation of mo-DCs in the context of M-CSF/IL-4/TNF-α stimulation, we analyzed whether a similar phenomenon might be observed in a more complex system. We analyzed the effect induced by low pH on whole peripheral blood mononuclear cells (PBMCs) stimulated by phytohemagglutinin (PHA) for 7 days and studied the phenotype of $CD11b^+$ cells within the monocyte/macrophage gate of the forward scatter/side scatter (FSC/SSC) dot plot. Cultures performed at pH 7.3 yielded two major cell populations ($CD14^-$ and $CD14^+$ cells), both of which were negative for CD1a expression. In contrast, cultures performed at pH 6.5 resulted in the differentiation of a population of $CD1a^+$ $CD14^-$ cells (Figure S2A) that expressed CD1c, HLA-DR, dendritic cell-specific intercellular adhesion molecule-3-grabbing non-integrin (DC-SIGN), and CD11c but not CD16 and CD64 (Figure S2B). We then analyzed the phenotypic changes induced by LPS stimulation. In these experiments, we used two cell populations as controls, namely, classical DCs differentiated from monocytes cultured with IL-4 and granulocyte macrophage colony-stimulating factor (GM-CSF) and macrophages differentiated from monocytes cultured with M-CSF. DCs differentiated from PHA-stimulated PBMCs cultured at pH 6.5 and classical DCs showed a similar maturation response after LPS stimulation, whereas monocyte-derived macrophages showed only minor phenotypic changes (Figure S2C). We also analyzed the ability of DCs to induce the proliferation of allogeneic CD4+ T cells. PHA-stimulated PBMCs were cultured for 7 days at pH 6.5, and $CD1a^+CD16^-$ cells were then sorted and activated for 24 h with LPS. Contrasting with the observations made with monocyte-derived macrophages, sorted $CD1a^+CD16^-$ cells triggered a proliferative response similar to that induced by classical DCs (Figure S2D).

Because serum is able to modulate monocyte function (Gogolak et al., 2007; Leslie et al., 2008), we analyzed if a similar phenomenon would be observed in cultures performed in serum-free medium. Monocytes were cultured for 5 days without cytokines at pH 6.5 or 7.3 in medium supplemented with 0.1% BSA. Under these conditions, we could recover only a fraction

Figure 1. Low pH Promotes the Differentiation of mo-DCs in the Context of M-CSF, TNF-α, and IL-4 Stimulation

(A–C) Isolated monocytes (5×10^5/ml) were cultured for 5 days at different pH values, in medium supplemented with 10% FCS, M-CSF (100 ng/ml), TNF-α (5 ng/ml), and IL-4 (30 ng/ml). Then, the expression of CD1a and CD16 was determined by flow cytometry (A–B), and cell morphology was analyzed by fluorescence microscopy (C).

(D) Monocytes were cultured as described in (A), in the absence or presence of stemregenin 1 (8 μM), 4,7-dimethyl-1, 10-phenanthroline (50 μM), or 5,11-dihydroindolo(3,2-b)carbazole-6-carboxaldehyde (FICZ, 65 nM). Then, the expression of CD1a, CD14, and CD16 was determined.

(E–I) Monocytes were cultured as described in (A). Then, cells were stimulated, or not, with LPS (20 ng/ml) for 24 h, and the expression of HLA-DR and CD86 (E, left panel), the production of cytokines (ELISA) (E, right panel), and cell ability to induce the proliferation (F–H) and the production of IFN-γ and IL-5 by allogeneic CD4+ T lymphocytes (I) were evaluated. A CD4+ T cell/antigen presenting cell ratio of 4:1 was used in (F), (H), and (I). In (G), different ratios of CD4+T cells: antigen presenting cells were used. Monocytes were cultured as described in (A). Then, $CD16^+$/$CD1a^-$ cells and $CD16^-$/$CD1a^+$ cells from cultures performed at pH 7.3 and $CD16^-$/$CD1a^+$ cells from cultures performed at pH 6.5 were sorted by fluorescence-activated cell sorting (FACS). Cells were treated with LPS (20 ng/ml) for 24 h, and their ability to induce the proliferation and the production of IFN-γ and IL-2 by allogeneic CD4+ T lymphocytes (CD4+ T cell/antigen presenting cell ratio of 4:1) were evaluated (J and K).

(L) Cells were cultured as described in (A), in the absence or presence of dexamethasone (100 nM) or PGE2 (100 nM). Then, the expression of CD1a and CD14 was evaluated. Representative experiments ($n = 3–15$) are shown in (A, left), (B), (C), (D, left), (F), and (J, left), and (L). In (A, right), (D, right), (E), (G), (H), (I), (J, right), and (K), results are expressed as the mean ± SEM of 4–6 different donors. *$p < 0.05$, **$p < 0.001$, and*** $p < 0.0001$; pH 7.3 versus pH 6.5.

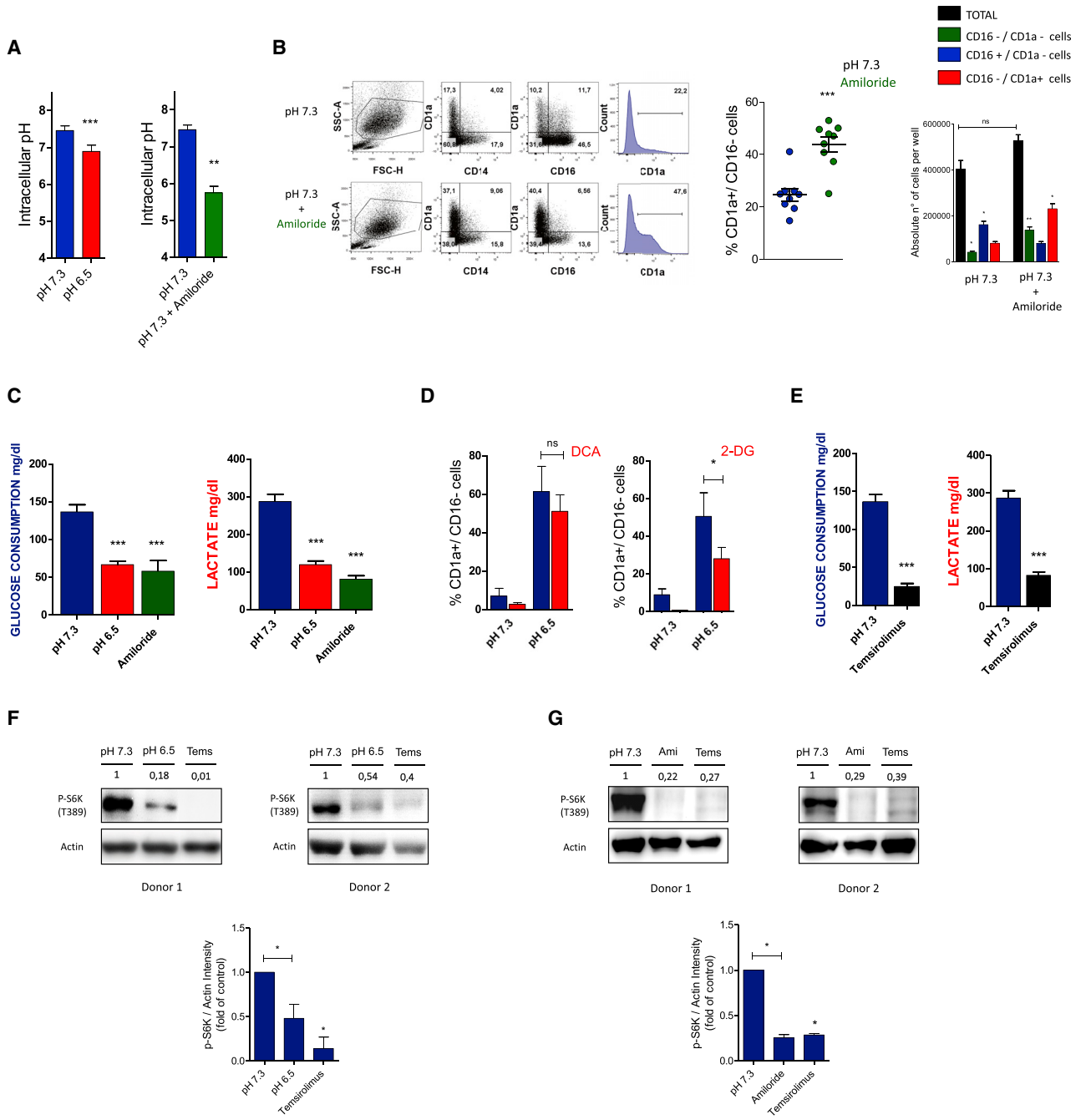

Figure 2. Low Extracellular pH Decreases Intracellular pH and Induces a Starvation-like Response

(A) Monocytes (5×10^5/ml) were loaded with the fluorescent dye BCECF-AM and cultured for 18 h in medium supplemented with 10% FCS, M-CSF (100 ng/ml), TNF-α (5 ng/ml), and IL-4 (30 ng/ml), at pH 7.3, pH 6.5 (left), or pH 7.3 in the presence of amiloride (100 μM) (right). Assessment of intracellular pH was performed as described in Materials and Methods.

(B) Monocytes (5×10^5/ml) were cultured for 5 days at pH 7.3 in medium supplemented with 10% FCS, M-CSF (100 ng/ml), TNF-α (5 ng/ml), and IL-4 (30 ng/ml), in the absence or presence of amiloride (100 μM). Then, the expression of CD1a, CD14, and CD16 was evaluated.

(C) Monocytes were cultured as described in (B), at pH 6.5 or pH 7.3. Then, glucose and lactate concentrations were determined by enzymatic methods.

(D) Monocytes were cultured as described in (C), in the absence or presence of DCA (dichloroacetate, 1 mM) or 2DG (2-deoxyglucose, 2 mM). Then, the expression of CD1a, CD14, and CD16 was evaluated.

(E) Monocytes were cultured as described in (C), in the absence or presence of temsirolimus (100 nM). Then, glucose and lactate concentrations were determined by enzymatic methods.

(legend continued on next page)

of the total number of seeded cells that was significantly higher for cultures performed at pH 6.than at pH 7.3 (Figure S2E). We found that cultures performed at pH 6.5, but not at pH 7.3, resulted in the differentiation of a population of DCs (Figure S2F) that increased the expression of HLA-DR and CD86 upon LPS stimulation (Figure S2G) and showed a high allostimulatory activity (Figure S2H). Notably, additional experiments performed in serum-free medium revealed that differentiation of monocytes into macrophages induced by M-CSF was redirected toward a DC-like phenotype when cultures were performed at pH 6.5 (Figure S2I). These DCs increased the expression of HLA-DR and CD86 upon LPS stimulation (Figure S2J) and showed a high allostimulatory activity (Figure S2K). We also analyzed the influence of acidosis on the differentiation of mo-DCs induced by GM-CSF and IL-4 in serum-supplemented medium (Sallusto and Lanzavecchia, 1994). Acidosis did not promote, but rather it partially inhibited ($p < 0.05$), the differentiation of mo-DCs (Figure S3).

Low pH Induces a Fall in Intracellular pH and a Starvation-like Response

High concentrations of protons modulate cell function by two major mechanisms: by interacting with different families of pH sensors expressed on the cell surface (Ishii et al., 2005; Liu et al., 2010; Ludwig et al., 2003; Radu et al., 2005; Tong et al., 2011) or by lowering cytosolic pH (Faucher and Naccache, 1987; Ritter et al., 1990; Simchowitz and Cragoe, 1986; Yuli and Oplatka, 1987). We found that exposure of monocytes to pH 6.5 resulted in a drop in cytoplasmic pH (Figure 2A, left). To analyze if a decrease in cytosolic pH might be responsible for the promotion of DC differentiation, we used the Na^+/H^+ exchanger (NHE) inhibitor amiloride. Consistent with the ability of NHE inhibitors to induce the cytosolic accumulation of protons (Kim et al., 1991), we found that amiloride profoundly decreased intracellular pH (Figure 2A, right). Moreover, it significantly promoted the differentiation of mo-DCs at pH 7.3 in the presence of M-CSF, IL-4, and TNF-α (Figure 2B). Quantification of the absolute number of cells in cultures performed in the presence of amiloride confirmed that the enrichment in $CD1a^+CD16^-$ cells reflected an enhanced differentiation of monocytes into DCs (Figure 2B, right panel). Promotion of DC differentiation induced by amiloride was completely prevented by the AHR inhibitor stemregenin-1 (Figure S4).

Previous studies in cell lines have shown that acidosis inhibits glycolysis (Corbet et al., 2016; Lamonte et al., 2013). We found that low pH as well as amiloride suppressed both glucose consumption and lactate production in monocytes cultured with M-CSF, IL-4, and TNF-α (Figure 2C). We hypothesized that inhibition of glycolysis might explain, at least partially, the ability of low pH to promote mo-DC differentiation. However, results in Figure 2D showed that two glycolytic inhibitors, 2-deoxy-D-glucose (2DG) and dichloroacetate (DCA), did not promote DC differentiation. In fact, 2DG partially prevented mo-DC differentiation, without affecting cell viability (data not shown). Studies performed in cell lines have shown that the starvation response induced by low pH involves not only the inhibition of glycolysis but also the inhibition of the cellular nutrient sensor mTORC1 (Balgi et al., 2011; Walton et al., 2018). As expected, we found that the mammalian target of rapamycin (mTOR) inhibitor temsirolimus markedly inhibited both glucose consumption and lactate production (Figure 2E). Interestingly, low pH and amiloride strongly inhibited mTORC1 activity (Figures 2F and 2G), raising the possibility that inhibition of mTORC1 might contribute to the ability of low pH to promote mo-DC differentiation.

mTORC1 Inhibition and Serum Starvation Promote the Differentiation of mo-DCs

We then analyzed whether mTORC1 inhibition was able to promote the differentiation of monocytes into DCs. Figure 3A shows that the mTORC1 inhibitor temsirolimus dramatically increased the differentiation of mo-DCs induced by M-CSF, IL-4, and TNF-α at pH 7.3. These mo-DCs showed a typical DC morphology (Figure 3B) and the ability to upregulate the expression of CD86 and HLA-DR (Figure 3C) as well as the production of IL-12 but not IL-10, IL-23, or IL-1β upon LPS stimulation (Figure 3D). Experiments performed with sorted cells indicated that temsirolimus mo-DCs showed a high ability to induce the proliferation of allogeneic T cells (Figure 3E) and the production of IL-2 and IFN-γ by alloreactive lymphocytes (Figure 3F). Interestingly, all these responses were induced at higher levels by temsirolimus mo-DCs than by control mo-DCs. Contrasting with the observations made in mo-DCs differentiated at pH 7.3 and pH 6.5 (see Figure 1D), we found that the differentiation of temsirolimus mo-DCs was not prevented by the AHR antagonist stemregenin-1, suggesting that it bypasses the participation of AHR (Figure S5).

Because serum activates mTOR, we hypothesized that cultures performed in serum-free medium might also promote DC differentiation. Decreasing serum concentrations from 10% to 1% promoted the differentiation of mo-DCs induced by M-CSF, IL-4, and TNF-α (Figure 3G). We could not assay serum-free conditions due to the high levels of cell death observed (not shown). It has been reported that GM-CSF promotes the differentiation of mo-DCs in cultures performed in serum-free conditions (Suzuki et al., 2004). We confirmed this previous finding (Figures 3H and 3I), and moreover, we observed that these DCs markedly increased CD86 expression and IL-12 production in response to LPS stimulation (Figure 3J), suggesting the acquisition of an inflammatory profile.

Transcriptomic Analysis of mo-DCs

To further characterize the properties of the different mo-DC populations arising from cultures performed at pH 7.3, pH 6.5, or pH 7.3 plus temsirolimus, RNA-seq analysis of

(F and G) Monocytes were cultured as described in (C) for 4 h at pH 7.3 in the absence or presence of temsirolimus (100nM) (F and G) or amiloride (100 μM) (G). Cells incubated for 4 h at pH 6.5 were also used (F). In all cases, cells were lysed and analyzed by SDS-PAGE and western blotting. Immunoblot analysis of the phosphorylation status of phospho(T389)-S6K using actin as a loading control was performed. Representative experiments (n = 3–6) are shown in (B, left), (F), and (G). Results are expressed as the mean ± SEM of 3–5 different donors in (A), (B, right), (C), (D), (E), (F) and (G). *$p < 0.05$, **$p < 0.001$, and ***$p < 0.0001$; versus pH 7.3.

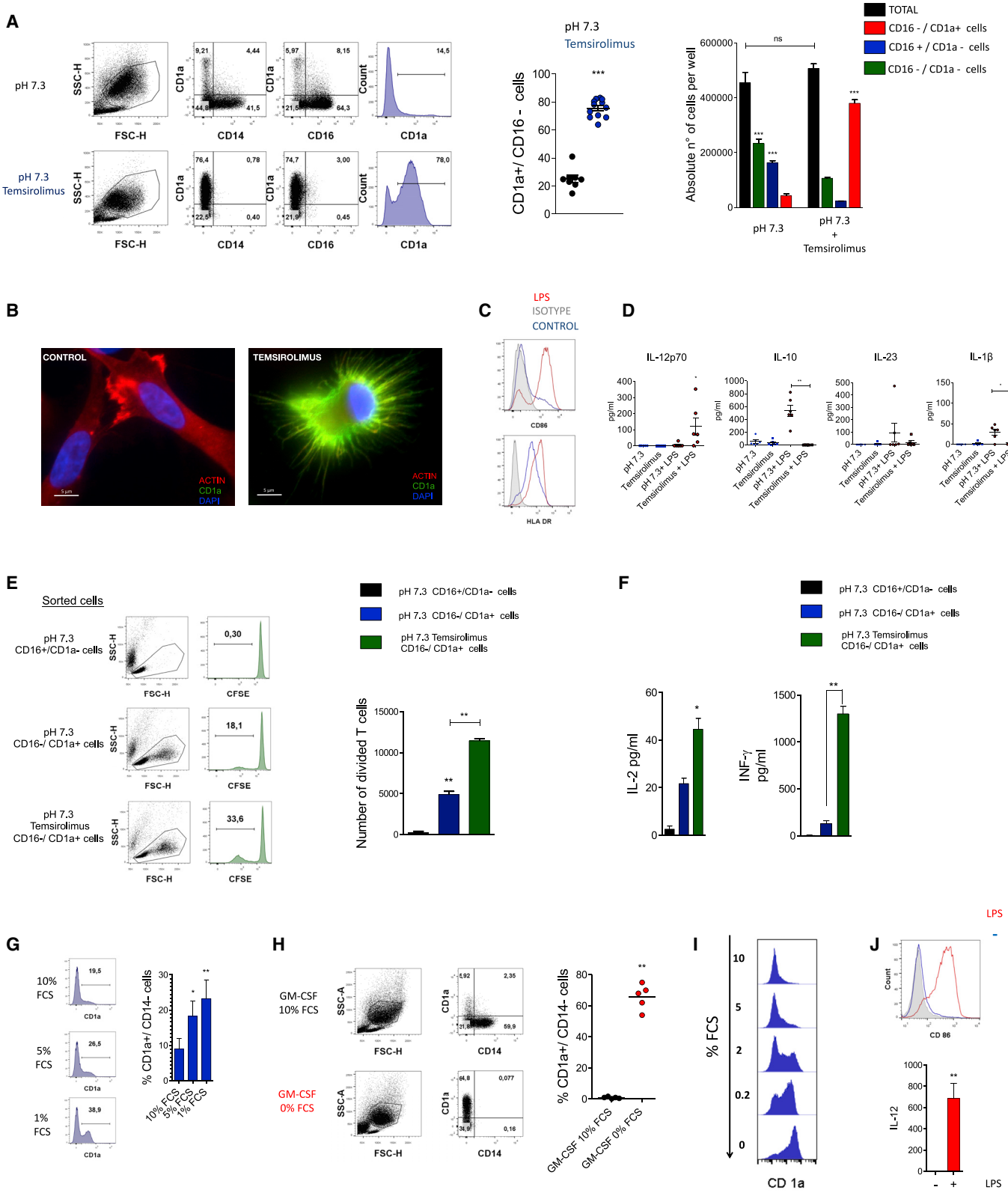

(legend on next page)

sorted CD1a$^+$CD16$^-$ cells was performed (Table S1; GEO: GSE143170). First, we analyzed whether CD1a$^+$CD16$^-$ cells obtained under these experimental conditions shared a common transcriptional signature associated with DC identity (Goudot et al., 2017; Segura et al., 2013). We found that CD1a$^+$CD16$^-$ cells from cultures performed at pH 7.3, pH 6.5, and pH 7.3 plus temsirolimus shared a high expression of DC-associated genes, such as *CD1A*, *CD1E*, *CD1B*, *FCεR1A*, *ITGAX* (CD11c), *CD209* (DC-SIGN), *CLEC10A*, *ZBTB46*, and *CD83*, and a low expression of macrophage-associated genes like *MERTK* and *CD163*. A heatmap representing the gene expression data of the selected genes is presented in Figure 4A (Table S2).

An analysis of the top 500 most variable genes (Figure 4B; Table S3) and principal-component analysis (PCA) analysis (Figure 4C) showed that mo-DCs obtained in the presence of temsirolimus clustered separately from mo-DCs obtained at pH 7.3 and pH 6.5. Temsirolimus mo-DCs, on the other hand, were shown to be enriched in the acquisition of more terminally differentiated and maturation genes, such as *CD1E*, *CD207* (Langerin), *FCER1A*, *OCLN*, *CLDN1*, *CCR7*, *HLA-DQ*, *TNFRSF4*, and *BIRC3* (Goudot et al., 2017; Jin et al., 2010; Matsunaga et al., 2002; Villani et al., 2017; Figure 4D; Table S4). Differential gene expression analysis between pH 6.5 and pH 7.3 mo-DCs showed the presence of 148 upregulated and 191 downregulated genes (Figure 4E; Table S5). Consistent with previous observations made in tumor cells (Corbet et al., 2016; Kondo et al., 2017), we found that pH 6.5 promoted the expression of genes associated with lipid metabolism and cholesterol biosynthesis (Figures 4E and 4F; Table S5). Also consistent with previous studies in tumor cells and neurons (Khacho et al., 2014; Wu et al., 2016; Xie et al., 2014), we found not only that mo-DCs differentiated at pH 6.5 upregulated genes of the mitochondrial respiratory chain (CI: *NDUFC1*, *NDUFS7;* CIII: *UQCRB*; CIV: *COX8A,COX6B1,NDUFA4*) (Figures 4E and 4F; Table S5) but also that the mitochondrial complex I inhibitor rotenone markedly induced apoptosis of monocytes cultured with M-CSF, TNF-α, and IL-4 at pH 6.5, but they exerted only minor effects at pH 7.3 (Figure S6). This suggests a critical role for mitochondrial respiration in the survival of mo-DCs differentiated at low pH values.

mTOR Inhibition Turns GM-CSF into a Strong Inducer of mo-DC Differentiation

GM-CSF promotes the differentiation of monocytes into macrophage-like cells in serum-supplemented medium (Lacey et al., 2012; Sander et al., 2017). We hypothesized that the inhibition of mTORC1 in monocytes might subvert the biological activity of GM-CSF, promoting the differentiation of mo-DCs. Figures 5A and 5B show that mTORC1 inhibition by temsirolimus effectively promoted a DC differentiation program in GM-CSF-treated monocytes. These mo-DCs increased the expression of CD86 and HLA-DR upon LPS stimulation in a similar fashion as classical DCs (Figure 5C). Notably, temsirolimus mo-DCs showed a higher production of IL-12 and a lower production of IL-10 upon LPS stimulation than classical DCs (Figure 5D). Moreover, temsirolimus mo-DCs displayed a strong ability to induce the proliferation of allogeneic T lymphocytes and the production of IFN-γ by alloreactive CD4+ T cells (Figures 5E and 5F).

DISCUSSION

Infiltration of peripheral tissues by monocytes is a common feature in the course of inflammatory processes and also occurs under steady-state conditions (Ingersoll et al., 2011). After entering tissues, monocytes can differentiate into macrophages or DCs (Cheong et al., 2010; Ginhoux and Jung, 2014; Randolph et al., 1999; van Furth and Cohn, 1968), but little is known about the environmental factors that determine this cell fate decision. Here, we show that low pH markedly promotes the differentiation of mo-DCs under different experimental conditions.

A large body of evidence from studies performed in cell lines show that acidic pH profoundly reprograms cellular metabolism from aerobic glycolysis toward fatty acid oxidation in the mitochondria (Corbet et al., 2016; Khacho et al., 2014; Lamonte et al., 2013). In line with these observations, we found not only that low pH inhibited glucose uptake and lactate production in the course of DC differentiation but also that monocytes cultured at low pH upregulated genes of the mitochondrial respiratory chain. Also consistent with observations made in cell lines (Balgi et al., 2011; Corbet

Figure 3. mTORC1 Inhibition and Serum Starvation Promote the Differentiation of mo-DCs

(A and B) Monocytes (5 × 10^5/ml) were cultured for 5 days at pH 7.3 in medium supplemented with 10% FCS, M-CSF (100 ng/ml), TNF-α (5 ng/ml), and IL-4 (30 ng/ml), in the absence or presence of temsirolimus (100 nM). The expression of CD1a, CD14, and CD16 was then evaluated (A), and cell morphology was analyzed by confocal microscopy (B).

(C and D). Monocytes were cultured as described in (A) and treated, or not, with LPS during 24 h. The surface expression of CD86 and HLA-DR was then evaluated by FACS (C). Secretion of IL12 , IL10, IL23, and IL1β was determined in the supernatants by ELISA(D).

(E and F) Monocytes were cultured as described in (A). Then, CD16$^+$/CD1a$^-$ and CD16$^-$/CD1a$^+$ cells from cultures performed at pH 7.3 and CD16$^-$/CD1a$^+$ cells from cultures performed at pH 7.3 in the presence of temsirolimus (100nM) were sorted by FACS. Cells were treated with LPS (20 ng/ml) for 24 h, and their ability to induce the proliferation (E) and the production of IFN-γ and IL-2 (F) by allogeneic CD4+ T lymphocytes (CD4 T cell/antigen presenting cell ratio of 4:1) were evaluated.

(G) Monocytes (5 × 10^5/ml) were cultured for 5 days at pH 7.3, in medium supplemented with different concentrations of FCS, in the presence of M-CSF, TNFα, and IL-4. Then, the expression of CD1a and CD14 was determined.

(H–J) Monocytes (5 × 10^5/ml) were cultured for 5 days in serum-free medium, in the presence of GM-CSF (50 ng/ml). FACS analysis of the recovered cells is presented in (H). A representative experiment using different concentrations of FCS is shown in (I). Then, cells recovered from cultures performed in serum-free medium were cultured for 24 h with or without LPS (20 ng/ml), and the expression of CD86 and the production of IL-12 were analyzed (J). Representative experiments are shown in (A, left), (B), (C, left), (E, left), (G, left), (H, left), (I), and (J, up). Results are expressed as the mean ± SEM of 3–6 different donors in (A, right), (D), (E, right), (F), (G, right), (H, right), and (J, low). *$p < 0.05$, **$p < 0.001$, and ***$p < 0.0001$; versus controls.

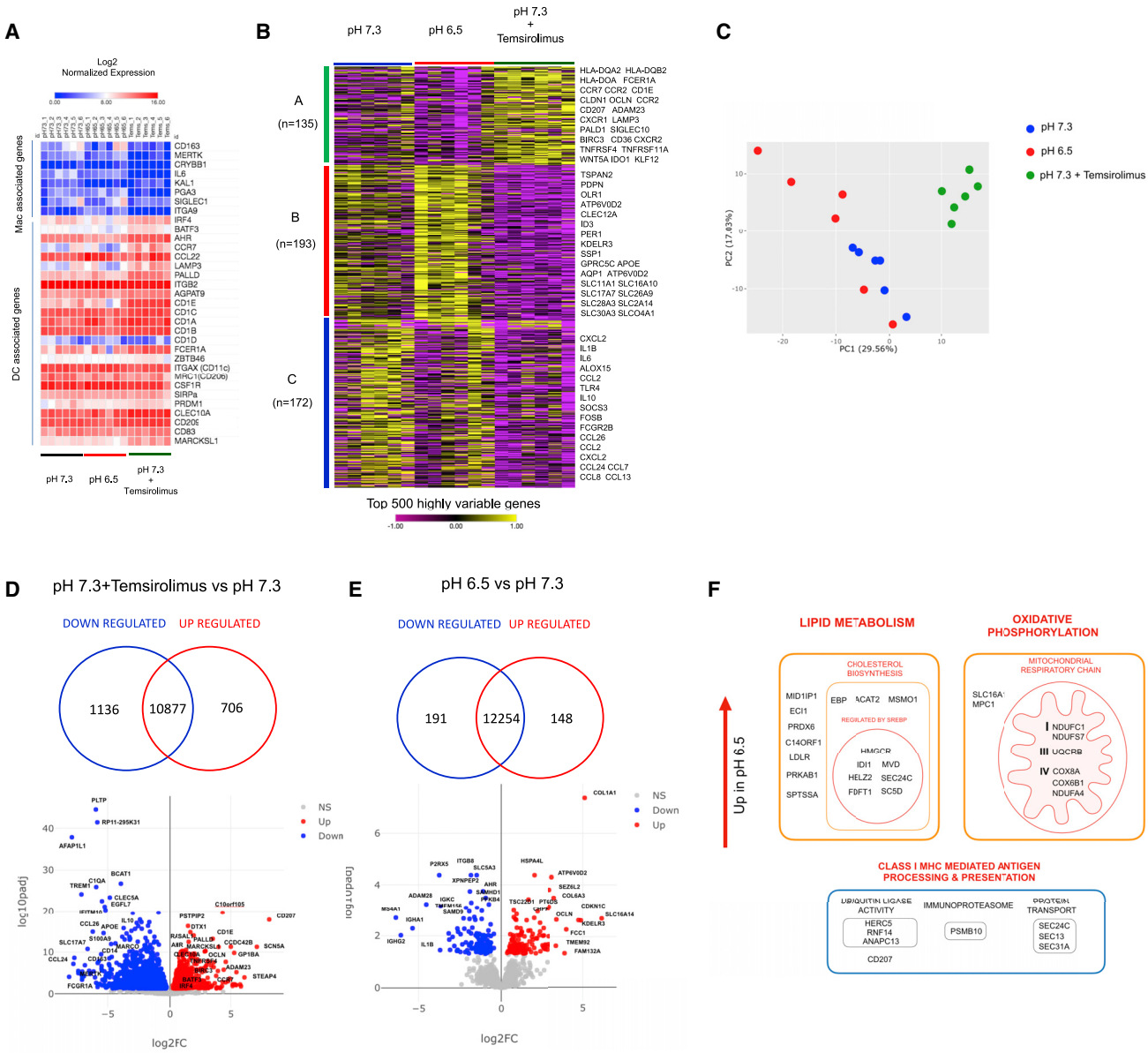

Figure 4. Transcriptomic Analysis of mo-DCs

(A–F) Monocytes were cultured in the presence of M-CSF (100 ng/ml), TNFα (5 ng/ml), and IL-4 (30 ng/ml) for 5 days at pH 7.3, pH 6.5, or pH 7.3 in the presence of temsirolimus (100 nM). Then, $CD1a^{+}CD16^{-}$ cells were sorted by FACS, and RNA was extracted for RNA-seq analysis (n = 6).

(A) Heatmap presenting the log2 normalized expression data of selected genes corresponding either to macrophage-associated or DC-associated signatures.

(B) Top 500 highly variable genes and K-means clustering.

(C) PCA analysis of the top 500 highly variable genes.

(D) Venn diagram and volcano plot of differentially expressed genes obtained using DESeq2 (false discovery rate [FDR] > 0.05, fold change [FC] > 1) (pH 7.3 + temsirolimus versus pH 7.3).

(E) Venn diagrams and volcano plots of differentially expressed genes obtained using DESeq2 (FDR > 0.05, FC > 1) (pH 6.5 versus pH 7.3).

(F) Schematic representation of up- and down-modulated groups of genes after pathway analysis (pH 6.5 versus pH 7.3).

et al., 2016; Lamonte et al., 2013; Walton et al., 2018), we found that low pH markedly inhibited the activity of mTORC1, a cellular nutrient sensor that plays an essential role in cell growth and survival (Kim and Guan, 2019; Saxton and Sabatini, 2017). Interestingly, the NHE inhibitor amiloride reproduced all the effects, suggesting that a drop in cytoplasmic pH might explain, at least partially, the ability of extracellular pH to promote mo-DC differentiation.

Here, we also reported that the mTORC1 inhibitor temsirolimus markedly promotes mo-DC differentiation. We found a similar response in different cytokine contexts, i.e., in the presence of M-CSF, IL-4, and TNF-α, as well in the presence of

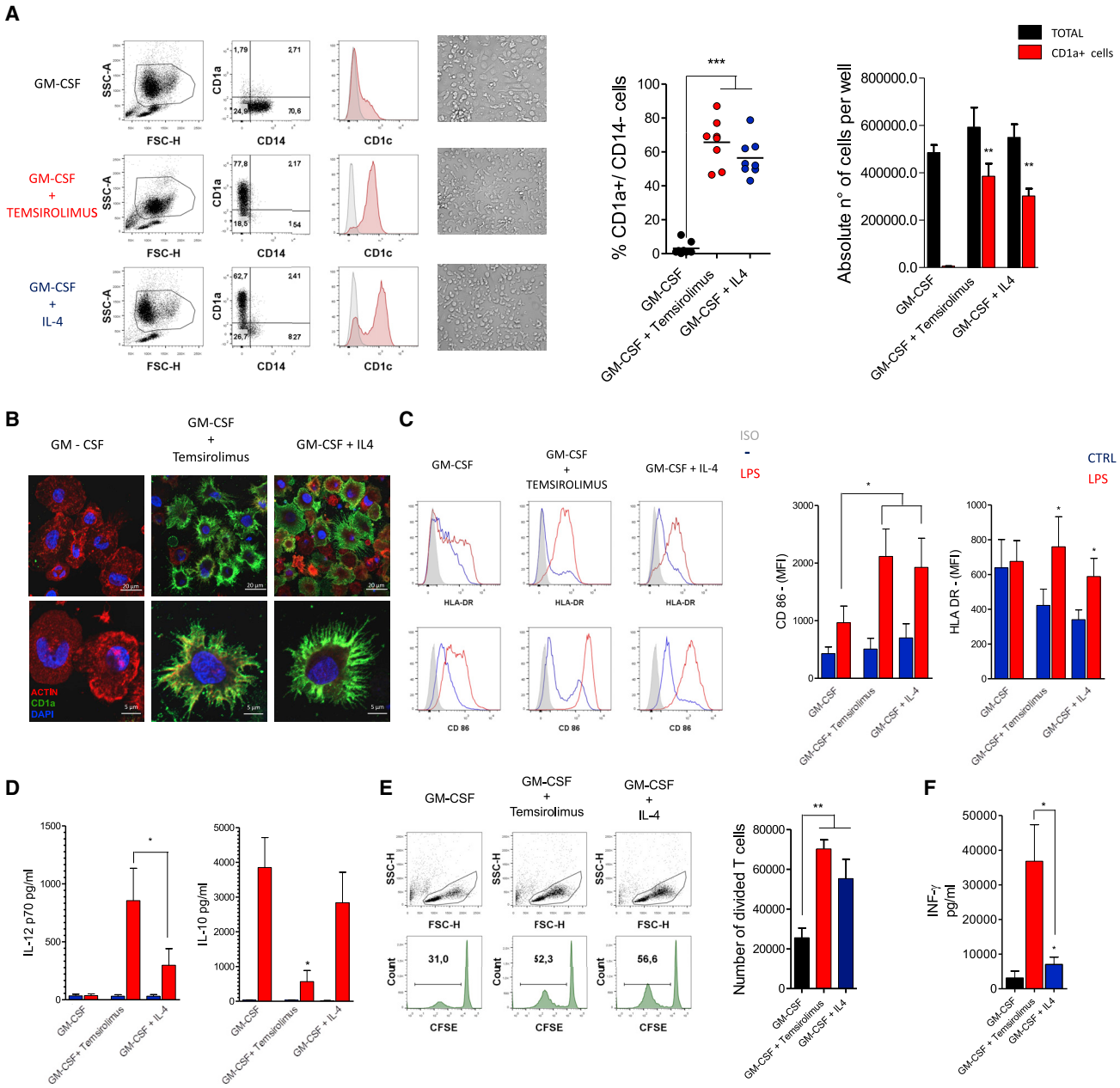

Figure 5. mTOR Inhibition Turns GM-CSF into a Strong Inducer of mo-DC Differentiation

(A and B) Monocytes (1×10^6/ml) were cultured for 5 days at pH 7.3 in medium supplemented with 10% FCS and GM-CSF (50 ng/ml), in the absence or presence of temsirolimus (100 nM). Then, the expression of CD1a, CD1c, and CD14 was determined (A), and cell morphology was analyzed by confocal microscopy (B). Classical DCs, obtained from monocytes cultured with GM-CSF and IL-4 were used as controls.

(C and D) Monocytes were cultured as described in (A) and treated, or not, with LPS during 24 h. Then, the phenotype (C) and the production of different cytokines were evaluated (D).

(E and F) Monocytes were cultured as described in (A) and treated, or not, with LPS during 24 h. Their ability to induce the proliferation (E) and the production of IFN-γ by allogeneic CD4+ T lymphocytes (CD4 T cell/antigen presenting cell ratio of 4:1) (F) was then evaluated. Representative experiments are shown in (A, left), (B), (C, left), and (E, left). Results are expressed as the mean ± SEM of 3–6 different donors in (A, right), (C, right), (D), (E, right), and (F). *$p < 0.05$, **$p < 0.001$, and ***$p < 0.0001$; versus controls.

GM-CSF. In contrast, and in agreement with previous results (Haidinger et al., 2010), we observed (data not shown) that inhibition of mTORC1 resulted in diminished cell viability in monocytes cultured with GM-CSF and IL-4. Together, these observations indicate that the role of mTOR in the differentiation of mo-DCs is strongly dependent on the cytokine environment.

Early studies identified mTORC1 inhibitors as immunosuppressive agents and were, thus, used to prevent allorejection in transplanted patients (Saunders et al., 2001; Thomson et al., 2009). More recent studies, however, suggested a more complex picture. Rapamycin-mediated inhibition of mTOR has been shown to increase CD8+ T cell memory (Araki et al., 2009; Diken et al., 2013; Ferrer et al., 2010; Li et al., 2012; Rao et al., 2010). Interestingly, Haidinger et al. (2010) reported divergent roles for mTOR on blood DCs and DCs derived from monocytes cultured with IL-4 and GM-CSF. Studies performed in murine models have shown that mTORC1 plays an important role in the development of different populations of DCs, such as the Flt3L-dependent CD8+ DC subset (Sathaliyawala et al., 2010) and Langerhans cells (Kellersch and Brocker, 2013; Sukhbaatar et al., 2016). Moreover, a number of studies showed that mTOR inhibition promotes an inflammatory signature by already differentiated DCs (Amiel et al., 2012; Jagannath and Bakhru, 2012; Weichhart et al., 2008; Mineharu et al., 2014). Our present results suggest that mTOR inhibition might contribute to inflammatory reactions not only by promoting the acquisition of an inflammatory signature by already differentiated DCs but also by inducing the differentiation of tissue-infiltrating monocytes into mo-DCs.

Despite that low pH markedly inhibited mTORC1 activity, our observations show a number of differences between the actions induced by low pH and the mTORC1 inhibitor temsirolimus. Transcriptomic analysis of DCs showed major differences. Moreover, the AHR antagonist stemregenin-1 completely prevented the differentiation of mo-DCs in the context of M-CSF/IL-4/TNF-α stimulation at pH 6.5 without affecting the differentiation of mo-DCs promoted by temsirolimus. Finally, temsirolimus strongly induced the differentiation of mo-DCs in the context of GM-CSF stimulation, whereas low pH did not exert any significant effect. Further studies are required to define the contribution of mTORC1 inhibition to the promoting effect of low pH on mo-DC differentiation.

The mechanisms through which mTORC1 inhibition promotes mo-DC differentiation remain to be elucidated. Different downstream effectors of the starvation response might be causally implicated. mTORC1 acts as a link between cell nutritional status and protein acetylation state (Wan et al., 2017; Wellen et al., 2009). Serum deprivation (Wellen et al., 2009) and mTORC1 inhibition (Wan et al., 2017) have been shown to promote major changes in mitochondrial and cytosolic protein acetylation patterns while inducing global histone deacetylation. Classical histone deacetylases (HDACs) and Sirtuins, a type III HDAC, directly modulate gene expression by deacetylating histones and regulating the acetylation pattern of a variety of non-histone proteins, thus impinging on several cellular processes (Yang and Seto, 2007; Yao and Yang, 2011). We hypothesize that the induction of a starvation response induced by either serum deprivation or mTORC1 inhibition might drive the differentiation of mo-DCs by promoting changes in the acetylation pattern of histones and non-histone proteins. Supporting this hypothesis, it has been reported that the differentiation of mo-DCs is dependent on the activity of HDACs (Chauvistré et al., 2014; Nencioni et al., 2007). Moreover, our transcriptomic analysis of temsirolimus mo-DCs revealed the upregulation of two HDACs, namely, HDAC-1 and the type III HDAC SIRT1, which have previously shown to play an important role in the modulation of DC function (Chauvistré et al., 2014; Owczarczyk et al., 2015; Reddy et al., 2008). Notably, previous observations have also shown not only that acidosis leads to a NAD^+-dependent increase in the activity of the histone deacetylases SIRT1 and SIRT6 but also that tumor acidosis accounts for a net increase in tumor sensitivity to SIRT1 inhibitors (Corbet et al., 2016; McBrian et al., 2013). We hypothesize that modulation of HDAC expression and activity might represent a final common pathway through which acidosis and mTORC1 inhibition promoted the differentiation of monocytes into DCs.

STAR★METHODS

Detailed methods are provided in the online version of this paper and include the following:

- KEY RESOURCES TABLE
- RESOURCE AVAILABILITY
  - Lead Contact
  - Materials Availability
  - Data and Code Availability
- EXPERIMENTAL MODEL AND SUBJECT DETAILS
  - Human blood samples
- METHOD DETAILS
  - Cell Isolation
  - Cell cultures
  - Flow cytometry & cell sorting
  - Fluorescence and confocal microscopy
  - Measurement of cytokines by ELISA
  - Mixed Lymphocyte Reaction
  - Measurement of intracellular pH
  - Analysis of glucose and lactate concentrations
  - Cell lysates and immunoblots
  - RNA-seq library preparation
  - RNA-seq analysis
  - Chemicals
- QUANTIFICATION AND STATISTICAL ANALYSIS
  - Statistical analysis

SUPPLEMENTAL INFORMATION

Supplemental Information can be found online at https://doi.org/10.1016/j.celrep.2020.107613.

ACKNOWLEDGMENTS

We deeply thank Gabriel Duette, Pehuén Pereyra-Gerber, and Augusto Varese for their technical assistance and scientific discussions. This work was supported by grants from the Agencia Nacional de Promocin Científica y Tecnológica, Argentina (PIDC 0010-2015 and PICT 2014-1578) and Universidad de Buenos Aires (UBA) (UBACyT 20020130100446BA) to J.G.; INSERM, Agence Nationale de la Recherche (ANR-17-CE15-0011-01 and ANR-10-IDEX-0001-02 PSL), Institut Curie (CIC IGR-Curie 1428), and European Union's Horizon 2020 research and innovation programme under the Marie Sklodowska-Curie grant agreement no. 799882. High-throughput sequencing performed with the ICGex NGS platform of the Institut Curie was supported by grants ANR-10-EQPX-03 (Equipex) and ANR-10-INBS-09-08 (France Génomique 25 Consortium) from the Agence Nationale de la Recherche ("Investissements d'Avenir" program), by the Cancerpole Ile-de-France, and by the SiRIC-Curie program SiRIC grant "INCa-DGOS-4654."

AUTHOR CONTRIBUTIONS

J.G. and F.E.D. designed the experiments and wrote the manuscript. F.E.D. performed most of the experiments and data analysis. V.O. performed western blotting assays, prepared slides for confocal microscopy, and participated in the analysis of transcriptomic data. A.M. participated in the generation of cDNA libraries for the RNA-seq. E.D. contributed to the design of the experiments and performed a number of assays by flow cytometry. I.M. performed ELISA assays and contributed to the elaboration of the manuscript. J.S. collaborated with the discussion of the results and the preparation of the manuscript. V.G.P. contributed with technical assistance in the experiments involving cell sorting. S.A. and E.S. analyzed the transcriptomic data, contributed to the design of the experiments, and collaborated with the preparation of the manuscript. J.G. supervised the project.

DECLARATION OF INTERESTS

The authors declare no conflict of interest.

Received: May 24, 2019
Revised: January 31, 2020
Accepted: April 14, 2020
Published: May 5, 2020

REFERENCES

Abbot, N.C., Spence, V.A., Swanson-Beck, J., Carnochan, F.M., Gibbs, J.H., and Lowe, J.G. (1990). Assessment of the respiratory metabolism in the skin from transcutaneous measurements of pO2 and pCO2: potential for non-invasive monitoring of response to tuberculin skin testing. Tubercle *71*, 15–22.

Amiel, E., Everts, B., Freitas, T.C., King, I.L., Curtis, J.D., Pearce, E.L., and Pearce, E.J. (2012). Inhibition of mechanistic target of rapamycin promotes dendritic cell activation and enhances therapeutic autologous vaccination in mice. J. Immunol. *189*, 2151–2158.

Andrews, S. (2010). FastQC.https://www.bioinformatics.babraham.ac.uk/projects/fastqc/.

Araki, K., Turner, A.P., Shaffer, V.O., Gangappa, S., Keller, S.A., Bachmann, M.F., Larsen, C.P., and Ahmed, R. (2009). mTOR regulates memory CD8 T-cell differentiation. Nature *460*, 108–112.

Ashby, B.S. (1966). pH studies in human malignant tumours. Lancet *2*, 312–315.

Balgi, A.D., Diering, G.H., Donohue, E., Lam, K.K., Fonseca, B.D., Zimmerman, C., Numata, M., and Roberge, M. (2011). Regulation of mTORC1 signaling by pH. PLoS One *6*, e21549.

Banchereau, J., and Steinman, R.M. (1998). Dendritic cells and the control of immunity. Nature *392*, 245–252.

Boltjes, A., and van Wijk, F. (2014). Human dendritic cell functional specialization in steady-state and inflammation. Front. Immunol. *5*, 131.

Bryant, R.E., Rashad, A.L., Mazza, J.A., and Hammond, D. (1980). beta-Lactamase activity in human pus. J. Infect. Dis. *142*, 594–601.

Chauvistré, H., Küstermann, C., Rehage, N., Klisch, T., Mitzka, S., Felker, P., Rose-John, S., Zenke, M., and Seré, K.M. (2014). Dendritic cell development requires histone deacetylase activity. Eur. J. Immunol. *44*, 2478–2488.

Cheong, C., Matos, I., Choi, J.H., Dandamudi, D.B., Shrestha, E., Longhi, M.P., Jeffrey, K.L., Anthony, R.M., Kluger, C., Nchinda, G., et al. (2010). Microbial stimulation fully differentiates monocytes to DC-SIGN/CD209(+) dendritic cells for immune T cell areas. Cell *143*, 416–429.

Chow, S., Hedley, D., and Tannock, I. (1996). Flow cytometric calibration of intracellular pH measurements in viable cells using mixtures of weak acids and bases. Cytometry *24*, 360–367.

Coillard, A., and Segura, E. (2019). In vivo differentiation of human monocytes. Front Immunol. *10*, 1907.

Corbet, C., and Feron, O. (2017). Tumour acidosis: from the passenger to the driver's seat. Nat. Rev. Cancer *17*, 577–593.

Corbet, C., Pinto, A., Martherus, R., Santiago de Jesus, J.P., Polet, F., and Feron, O. (2016). Acidosis Drives the Reprogramming of Fatty Acid Metabolism in Cancer Cells through Changes in Mitochondrial and Histone Acetylation. Cell Metab. *24*, 311–323.

Diken, M., Kreiter, S., Vascotto, F., Selmi, A., Attig, S., Diekmann, J., Huber, C., Türeci, Ö., and Sahin, U. (2013). mTOR inhibition improves antitumor effects of vaccination with antigen-encoding RNA. Cancer Immunol. Res. *1*, 386–392.

Dubos, R.J. (1955). The micro-environment of inflammation or Metchnikoff revisited. Lancet *269*, 1–5.

Edlow, D.W., and Sheldon, W.H. (1971). The pH of inflammatory exudates. Proc. Soc. Exp. Biol. Med. *137*, 1328–1332.

Faucher, N., and Naccache, P.H. (1987). Relationship between pH, sodium, and shape changes in chemotactic-factor-stimulated human neutrophils. J. Cell. Physiol. *132*, 483–491.

Ferrer, I.R., Wagener, M.E., Robertson, J.M., Turner, A.P., Araki, K., Ahmed, R., Kirk, A.D., Larsen, C.P., and Ford, M.L. (2010). Cutting edge: Rapamycin augments pathogen-specific but not graft-reactive CD8+ T cell responses. J. Immunol. *185*, 2004–2008.

Ge, S.X., Son, E.W., and Yao, R. (2018). iDEP: an integrated web application for differential expression and pathway analysis of RNA-Seq data. BMC Bioinformatics *19*, 534.

Ge, S.X., Jung, D., and Yao, R. (2019). ShinyGO: a graphical enrichment tool for animals and plants. Bioinformatics, btz931.

Geborek, P., Saxne, T., Pettersson, H., and Wollheim, F.A. (1989). Synovial fluid acidosis correlates with radiological joint destruction in rheumatoid arthritis knee joints. J. Rheumatol. *16*, 468–472.

Geissmann, F., Manz, M.G., Jung, S., Sieweke, M.H., Merad, M., and Ley, K. (2010). Development of monocytes, macrophages, and dendritic cells. Science *327*, 656–661.

Ginhoux, F., and Jung, S. (2014). Monocytes and macrophages: developmental pathways and tissue homeostasis. Nat. Rev. Immunol. *14*, 392–404.

Gogolak, P., Rethi, B., Szatmari, I., Lanyi, A., Dezso, B., Nagy, L., and Rajnavolgyi, E. (2007). Differentiation of CD1a- and CD1a+ monocyte-derived dendritic cells is biased by lipid environment and PPARgamma. Blood *109*, 643–652.

Goudot, C., Coillard, A., Villani, A.C., Gueguen, P., Cros, A., Sarkizova, S., Tang-Huau, T.L., Bohec, M., Baulande, S., Hacohen, N., et al. (2017). Aryl Hydrocarbon Receptor Controls Monocyte Differentiation into Dendritic Cells versus Macrophages. Immunity *47*, 582–596.e586.

Greter, M., Helft, J., Chow, A., Hashimoto, D., Mortha, A., Agudo-Cantero, J., Bogunovic, M., Gautier, E.L., Miller, J., Leboeuf, M., et al. (2012). GM-CSF controls nonlymphoid tissue dendritic cell homeostasis but is dispensable for the differentiation of inflammatory dendritic cells. Immunity *36*, 1031–1046.

Guilliams, M., Ginhoux, F., Jakubzick, C., Naik, S.H., Onai, N., Schraml, B.U., Segura, E., Tussiwand, R., and Yona, S. (2014). Dendritic cells, monocytes and macrophages: a unified nomenclature based on ontogeny. Nat. Rev. Immunol. *14*, 571–578.

Haidinger, M., Poglitsch, M., Geyeregger, R., Kasturi, S., Zeyda, M., Zlabinger, G.J., Pulendran, B., Hörl, W.H., Säemann, M.D., and Weichhart, T. (2010). A versatile role of mammalian target of rapamycin in human dendritic cell function and differentiation. J. Immunol. *185*, 3919–3931.

Hawiger, D., Inaba, K., Dorsett, Y., Guo, M., Mahnke, K., Rivera, M., Ravetch, J.V., Steinman, R.M., and Nussenzweig, M.C. (2001). Dendritic cells induce peripheral T cell unresponsiveness under steady state conditions in vivo. J. Exp. Med. *194*, 769–779.

Helmlinger, G., Yuan, F., Dellian, M., and Jain, R.K. (1997). Interstitial pH and pO2 gradients in solid tumors in vivo: high-resolution measurements reveal a lack of correlation. Nat. Med. *3*, 177–182.

Ingersoll, M.A., Platt, A.M., Potteaux, S., and Randolph, G.J. (2011). Monocyte trafficking in acute and chronic inflammation. Trends Immunol. *32*, 470–477.

Ishii, S., Kihara, Y., and Shimizu, T. (2005). Identification of T cell death-associated gene 8 (TDAG8) as a novel acid sensing G-protein-coupled receptor. J. Biol. Chem. *280*, 9083–9087.

Jagannath, C., and Bakhru, P. (2012). Rapamycin-induced enhancement of vaccine efficacy in mice. Methods Mol. Biol. *821*, 295–303.

Jancic, C.C., Cabrini, M., Gabelloni, M.L., Rodríguez Rodrigues, C., Salamone, G., Trevani, A.S., and Geffner, J. (2012). Low extracellular pH stimulates the production of IL-1β by human monocytes. Cytokine *57*, 258–268.

Jin, P., Han, T.H., Ren, J., Saunders, S., Wang, E., Marincola, F.M., and Stroncek, D.F. (2010). Molecular signatures of maturing dendritic cells: implications for testing the quality of dendritic cell therapies. J. Transl. Med. *8*, 4.

Kaliński, P., Hilkens, C.M., Snijders, A., Snijdewint, F.G., and Kapsenberg, M.L. (1997). IL-12-deficient dendritic cells, generated in the presence of prostaglandin E2, promote type 2 cytokine production in maturing human naive T helper cells. J. Immunol. *159*, 28–35.

Kellersch, B., and Brocker, T. (2013). Langerhans cell homeostasis in mice is dependent on mTORC1 but not mTORC2 function. Blood *121*, 298–307.

Khacho, M., Tarabay, M., Patten, D., Khacho, P., MacLaurin, J.G., Guadagno, J., Bergeron, R., Cregan, S.P., Harper, M.E., Park, D.S., and Slack, R.S. (2014). Acidosis overrides oxygen deprivation to maintain mitochondrial function and cell survival. Nat. Commun. *5*, 3550.

Kim, J., and Guan, K.L. (2019). mTOR as a central hub of nutrient signalling and cell growth. Nat. Cell Biol. *21*, 63–71.

Kim, G.E., Lyons, J.C., and Song, C.W. (1991). Effects of amiloride on intracellular pH and thermosensitivity. Int. J. Radiat. Oncol. Biol. Phys. *20*, 541–549.

Kondo, A., Yamamoto, S., Nakaki, R., Shimamura, T., Hamakubo, T., Sakai, J., Kodama, T., Yoshida, T., Aburatani, H., and Osawa, T. (2017). Extracellular Acidic pH Activates the Sterol Regulatory Element-Binding Protein 2 to Promote Tumor Progression. Cell Rep. *18*, 2228–2242.

Kucukural, A., Yukselen, O., Ozata, D.M., Moore, M.J., and Garber, M. (2019). DEBrowser: interactive differential expression analysis and visualization tool for count data. BMC Genomics *20*, 6.

Lacey, D.C., Achuthan, A., Fleetwood, A.J., Dinh, H., Roiniotis, J., Scholz, G.M., Chang, M.W., Beckman, S.K., Cook, A.D., and Hamilton, J.A. (2012). Defining GM-CSF- and macrophage-CSF-dependent macrophage responses by in vitro models. J. Immunol. *188*, 5752–5765.

Lamonte, G., Tang, X., Chen, J.L., Wu, J., Ding, C.K., Keenan, M.M., Sangokoya, C., Kung, H.N., Ilkayeva, O., Boros, L.G., et al. (2013). Acidosis induces reprogramming of cellular metabolism to mitigate oxidative stress. Cancer Metab. *1*, 23.

Leslie, D.S., Dascher, C.C., Cembrola, K., Townes, M.A., Hava, D.L., Hugendubler, L.C., Mueller, E., Fox, L., Roura-Mir, C., Moody, D.B., et al. (2008). Serum lipids regulate dendritic cell CD1 expression and function. Immunology *125*, 289–301.

Li, Q., Rao, R., Vazzana, J., Goedegebuure, P., Odunsi, K., Gillanders, W., and Shrikant, P.A. (2012). Regulating mammalian target of rapamycin to tune vaccination-induced CD8(+) T cell responses for tumor immunity. J. Immunol. *188*, 3080–3087.

Liu, J.P., Nakakura, T., Tomura, H., Tobo, M., Mogi, C., Wang, J.Q., He, X.D., Takano, M., Damirin, A., Komachi, M., et al. (2010). Each one of certain histidine residues in G-protein-coupled receptor GPR4 is critical for extracellular proton-induced stimulation of multiple G-protein-signaling pathways. Pharmacol. Res. *61*, 499–505.

Love, M.I., Huber, W., and Anders, S. (2014). Moderated estimation of fold change and dispersion for RNA-seq data with DESeq2. Genome Biol. *15*, 550.

Ludwig, M.G., Vanek, M., Guerini, D., Gasser, J.A., Jones, C.E., Junker, U., Hofstetter, H., Wolf, R.M., and Seuwen, K. (2003). Proton-sensing G-protein-coupled receptors. Nature *425*, 93–98.

Månsson, B., Geborek, P., Saxne, T., and Björnsson, S. (1990). Cytidine deaminase activity in synovial fluid of patients with rheumatoid arthritis: relation to lactoferrin, acidosis, and cartilage proteoglycan release. Ann. Rheum. Dis. *49*, 594–597.

Matsunaga, T., Ishida, T., Takekawa, M., Nishimura, S., Adachi, M., and Imai, K. (2002). Analysis of gene expression during maturation of immature dendritic cells derived from peripheral blood monocytes. Scand. J. Immunol. *56*, 593–601.

McBrian, M.A., Behbahan, I.S., Ferrari, R., Su, T., Huang, T.W., Li, K., Hong, C.S., Christofk, H.R., Vogelauer, M., Seligson, D.B., and Kurdistani, S.K. (2013). Histone acetylation regulates intracellular pH. Mol. Cell *49*, 310–321.

Menck, K., Behme, D., Pantke, M., Reiling, N., Binder, C., Pukrop, T., and Klemm, F. (2014). Isolation of human monocytes by double gradient centrifugation and their differentiation to macrophages in teflon-coated cell culture bags. J. Vis. Exp., e51554.

Merad, M., Sathe, P., Helft, J., Miller, J., and Mortha, A. (2013). The dendritic cell lineage: ontogeny and function of dendritic cells and their subsets in the steady state and the inflamed setting. Annu. Rev. Immunol. *31*, 563–604.

Mildner, A., and Jung, S. (2014). Development and function of dendritic cell subsets. Immunity *40*, 642–656.

Mineharu, Y., Kamran, N., Lowenstein, P.R., and Castro, M.G. (2014). Blockade of mTOR signaling via rapamycin combined with immunotherapy augments antiglioma cytotoxic and memory T-cell functions. Mol. Cancer Ther. *13*, 3024–3036.

Nencioni, A., Beck, J., Werth, D., Grunebach, F., Patrone, F., Ballestrero, A., and Brossart, P. (2007). Histone deacetylase inhibitors affect dendritic cell differentiation and immunogenicity. Clin. Cancer Res. *13*, 3933–3941.

Obermajer, N., Muthuswamy, R., Lesnock, J., Edwards, R.P., and Kalinski, P. (2011). Positive feedback between PGE2 and COX2 redirects the differentiation of human dendritic cells toward stable myeloid-derived suppressor cells. Blood *118*, 5498–5505.

Owczarczyk, A.B., Schaller, M.A., Reed, M., Rasky, A.J., Lombard, D.B., and Lukacs, N.W. (2015). Sirtuin 1 Regulates Dendritic Cell Activation and Autophagy during Respiratory Syncytial Virus-Induced Immune Responses. J. Immunol. *195*, 1637–1646.

Patro, R., Duggal, G., Love, M.I., Irizarry, R.A., and Kingsford, C. (2017). Salmon provides fast and bias-aware quantification of transcript expression. Nat. Methods *14*, 417–419.

Radu, C.G., Nijagal, A., McLaughlin, J., Wang, L., and Witte, O.N. (2005). Differential proton sensitivity of related G protein-coupled receptors T cell death-associated gene 8 and G2A expressed in immune cells. Proc. Natl. Acad. Sci. USA *102*, 1632–1637.

Randolph, G.J., Inaba, K., Robbiani, D.F., Steinman, R.M., and Muller, W.A. (1999). Differentiation of phagocytic monocytes into lymph node dendritic cells in vivo. Immunity *11*, 753–761.

Rao, R.R., Li, Q., Odunsi, K., and Shrikant, P.A. (2010). The mTOR kinase determines effector versus memory CD8+ T cell fate by regulating the expression of transcription factors T-bet and Eomesodermin. Immunity *21*, 67–78.

Reddy, P., Sun, Y., Toubai, T., Duran-Struuck, R., Clouthier, S.G., Weisiger, E., Maeda, Y., Tawara, I., Krijanovski, O., Gatza, E., et al. (2008). Histone deacetylase inhibition modulates indoleamine 2,3-dioxygenase-dependent DC functions and regulates experimental graft-versus-host disease in mice. J. Clin. Invest. *118*, 2562–2573.

Richter, L., Landsverk, O.J.B., Atlasy, N., Bujko, A., Yaqub, S., Horneland, R., Øyen, O., Aandahl, E.M., Lundin, K.E.A., Stunnenberg, H.G., et al. (2018). Transcriptional profiling reveals monocyte-related macrophages phenotypically resembling DC in human intestine. Mucosal Immunol. *11*, 1512–1523.

Ritter, J.M., Doktor, H.S., and Benjamin, N. (1990). Paradoxical effect of bicarbonate on cytoplasmic pH. Lancet *335*, 1243–1246.

Sallusto, F., and Lanzavecchia, A. (1994). Efficient presentation of soluble antigen by cultured human dendritic cells is maintained by granulocyte/macrophage colony-stimulating factor plus interleukin 4 and downregulated by tumor necrosis factor alpha. J. Exp. Med. *179*, 1109–1118.

Sander, J., Schmidt, S.V., Cirovic, B., McGovern, N., Papantonopoulou, O., Hardt, A.L., Aschenbrenner, A.C., Kreer, C., Quast, T., Xu, A.M., et al. (2017). Cellular Differentiation of Human Monocytes Is Regulated by Time-Dependent Interleukin-4 Signaling and the Transcriptional Regulator NCOR2. Immunity *47*, 1051–1066.e1012.

Sathaliyawala, T., O'Gorman, W.E., Greter, M., Bogunovic, M., Konjufca, V., Hou, Z.E., Nolan, G.P., Miller, M.J., Merad, M., and Reizis, B. (2010).

Mammalian target of rapamycin controls dendritic cell development downstream of Flt3 ligand signaling. Immunity *33*, 597–606.

Saunders, R.N., Metcalfe, M.S., and Nicholson, M.L. (2001). Rapamycin in transplantation: a review of the evidence. Kidney Int. *59*, 3–16.

Saxton, R.A., and Sabatini, D.M. (2017). mTOR Signaling in Growth, Metabolism, and Disease. Cell *169*, 361–371.

Schneider, C.A., Rasband, W.S., and Eliceiri, K.W. (2012). NIH Image to ImageJ: 25 years of image analysis. Nat. Methods *9*, 671–675.

Segura, E., and Amigorena, S. (2013). Inflammatory dendritic cells in mice and humans. Trends Immunol. *34*, 440–445.

Segura, E., Touzot, M., Bohineust, A., Cappuccio, A., Chiocchia, G., Hosmalin, A., Dalod, M., Soumelis, V., and Amigorena, S. (2013). Human inflammatory dendritic cells induce Th17 cell differentiation. Immunity *38*, 336–348.

Shortman, K., and Naik, S.H. (2007). Steady-state and inflammatory dendritic-cell development. Nat. Rev. Immunol. *7*, 19–30.

Simchowitz, L., and Cragoe, E.J., Jr. (1986). Regulation of human neutrophil chemotaxis by intracellular pH. J. Biol. Chem. *261*, 6492–6500.

Simmen, H.P., and Blaser, J. (1993). Analysis of pH and pO2 in abscesses, peritoneal fluid, and drainage fluid in the presence or absence of bacterial infection during and after abdominal surgery. Am. J. Surg. *166*, 24–27.

Simmen, H.P., Battaglia, H., Giovanoli, P., and Blaser, J. (1994). Analysis of pH, pO2 and pCO2 in drainage fluid allows for rapid detection of infectious complications during the follow-up period after abdominal surgery. Infection *22*, 386–389.

Soneson, C., Love, M.I., and Robinson, M.D. (2015). Differential analyses for RNA-seq: transcript-level estimates improve gene-level inferences. F1000Res. *4*, 1521.

Sukhbaatar, N., Hengstschläger, M., and Weichhart, T. (2016). mTOR-Mediated Regulation of Dendritic Cell Differentiation and Function. Trends Immunol. *37*, 778–789.

Suzuki, H., Katayama, N., Ikuta, Y., Mukai, K., Fujieda, A., Mitani, H., Araki, H., Miyashita, H., Hoshino, N., Nishikawa, H., et al. (2004). Activities of granulocyte-macrophage colony-stimulating factor and interleukin-3 on monocytes. Am. J. Hematol. *75*, 179–189.

Tamoutounour, S., Guilliams, M., Montanana Sanchis, F., Liu, H., Terhorst, D., Malosse, C., Pollet, E., Ardouin, L., Luche, H., Sanchez, C., et al. (2013). Origins and functional specialization of macrophages and of conventional and monocyte-derived dendritic cells in mouse skin. Immunity *39*, 925–938.

Thomson, A.W., Turnquist, H.R., and Raimondi, G. (2009). Immunoregulatory functions of mTOR inhibition. Nat. Rev. Immunol. *9*, 324–337.

Tong, J., Wu, W.N., Kong, X., Wu, P.F., Tian, L., Du, W., Fang, M., Zheng, F., Chen, J.G., Tan, Z., and Gong, F. (2011). Acid-sensing ion channels contribute to the effect of acidosis on the function of dendritic cells. J. Immunol. *186*, 3686–3692.

van Furth, R., and Cohn, Z.A. (1968). The origin and kinetics of mononuclear phagocytes. J. Exp. Med. *128*, 415–435.

Villani, A.C., Satija, R., Reynolds, G., Sarkizova, S., Shekhar, K., Fletcher, J., Griesbeck, M., Butler, A., Zheng, S., Lazo, S., et al. (2017). Single-cell RNA-seq reveals new types of human blood dendritic cells, monocytes, and progenitors. Science *356*, eaah4573.

Walton, Z.E., Patel, C.H., Brooks, R.C., Yu, Y., Ibrahim-Hashim, A., Riddle, M., Porcu, A., Jiang, T., Ecker, B.L., Tameire, F., et al. (2018). Acid Suspends the Circadian Clock in Hypoxia through Inhibition of mTOR. Cell *174*, 72–87.e32.

Wan, W., You, Z., Xu, Y., Zhou, L., Guan, Z., Peng, C., Wong, C.C.L., Su, H., Zhou, T., Xia, H., et al. (2017). mTORC1 Phosphorylates Acetyltransferase p300 to Regulate Autophagy and Lipogenesis. Mol. Cell *68*, 323–335.e326.

Weichhart, T., Costantino, G., Poglitsch, M., Rosner, M., Zeyda, M., Stuhlmeier, K.M., Kolbe, T., Stulnig, T.M., Hörl, W.H., Hengstschläger, M., et al. (2008). The TSC-mTOR signaling pathway regulates the innate inflammatory response. Immunity *29*, 565–577.

Wellen, K.E., Hatzivassiliou, G., Sachdeva, U.M., Bui, T.V., Cross, J.R., and Thompson, C.B. (2009). ATP-citrate lyase links cellular metabolism to histone acetylation. Science *324*, 1076–1080.

Woltman, A.M., de Fijter, J.W., Kamerling, S.W., Paul, L.C., Daha, M.R., and van Kooten, C. (2000). The effect of calcineurin inhibitors and corticosteroids on the differentiation of human dendritic cells. Eur. J. Immunol. *30*, 1807–1812.

Wu, H., Ying, M., and Hu, X. (2016). Lactic acidosis switches cancer cells from aerobic glycolysis back to dominant oxidative phosphorylation. Oncotarget *7*, 40621–40629.

Xie, J., Wu, H., Dai, C., Pan, Q., Ding, Z., Hu, D., Ji, B., Luo, Y., and Hu, X. (2014). Beyond Warburg effect–dual metabolic nature of cancer cells. Sci. Rep. *4*, 4927.

Yang, X.J., and Seto, E. (2007). HATs and HDACs: from structure, function and regulation to novel strategies for therapy and prevention. Oncogene *26*, 5310–5318.

Yao, Y.L., and Yang, W.M. (2011). Beyond histone and deacetylase: an overview of cytoplasmic histone deacetylases and their nonhistone substrates. J. Biomed. Biotechnol. *2011*, 146493.

Yuli, I., and Oplatka, A. (1987). Cytosolic acidification as an early transductory signal of human neutrophil chemotaxis. Science *235*, 340–342.

STAR★METHODS

KEY RESOURCES TABLE

REAGENT or RESOURCE	SOURCE	IDENTIFIER
Antibodies		
APC Mouse Anti-Human CD1a	BD Biosciences	Cat# 559775, RRID:AB_398669
FITC Mouse Anti-Human CD1a	BD Biosciences	Cat #555806, RRID:AB_396140
BV421 Mouse Anti-Human CD14	BD Biosciences	Cat # 563743, RRID:AB_2744289
FITC Mouse Anti-Human CD14	BD Biosciences	Cat # 555397, RRID:AB_395798
PE Mouse Anti-Human CD14	BD Biosciences	Cat # 555398, RRID:AB_395799
PE Mouse Anti-Human CD16	BD Biosciences	Cat # 347617, RRID:AB_400331
FITC Mouse Anti-Human CD64	BD Biosciences	Cat # 555527, RRID:AB_395913
APC Mouse Anti-Human CD209	BD Biosciences	Cat # 551545, RRID:AB_647161
PE Mouse Anti-Human CD1c	BD Biosciences	Cat # 564900, RRID:AB_2739006
PE Mouse Anti-Human CD86	BD Biosciences	Cat # 555658, RRID:AB_396013
FITC Mouse Anti-Human CD80	BD Biosciences	Cat # 560926, RRID:AB_396605
FITC Mouse Anti-Human HLA-DR	BD Biosciences	Cat # 555811, RRID:AB_396145
APC-Cy7 Mouse Anti-Human HLA-DR	BD Biosciences	Cat # 335796, RRID:AB_399974
APC-Cy7 Mouse Anti-Human CD11b	BD Biosciences	Cat# 557754, RRID:AB_2033935
APC Mouse Anti-Human CD11C	BD Biosciences	Cat# 559877, RRID:AB_398680
Purified Mouse Anti-Human CD1a	BD Biosciences	Cat#555805, RRID:AB_396139
Alexa Fluor® 488 AffiniPure Donkey Anti-Mouse IgG (H+L)	Jackson ImmunoResearch	Cat# 715545150, RRID:AB_2341099
Phospho-p70 S6 Kinase (Thr389) Antibody	Cell Signaling	Cat# 9205, RRID:AB_2734746
beta Actin Loading Control Monoclonal Antibody (BA3R)	Invitrogen	Cat# MA5-15739, RRID:AB_10979409
Peroxidase AffiniPure Goat Anti-Rabbit IgG (H+L)	Jackson ImmunoResearch	Cat# 111-035-144, RRID:AB_2307391
Peroxidase AffiniPure Goat Anti-Mouse IgG (H+L)	Jackson ImmunoResearch	Cat# 115-035-003, RRID:AB_10015289
Chemicals, Peptides, and Recombinant Proteins		
Alexa Fluor 594 Phalloidin	Invitrogen	Cat# A12381
L-PHA (L-Phytohemagglutinin)	Sigma-Aldrich	Cat# L2769
7AAD	BD Biosciences	Cat# 559925
FITC Annexin V	BD Biosciences	Cat# 556419
BCECF, AM (2′,7′-Bis-(2-Carboxyethyl)-5-(and-6)-Carboxyfluorescein, Acetoxymethyl Ester)	Invitrogen	Cat# B1170
eBioscience CFSE	Invitrogen	Cat# 65-0850-84
DAPI Fluoromount-G®	Southern Biotech	Cat# 0100-20
Bovine serum albumin	DFS Labs (Argentina)	BSA Standard
Amiloride hydrochloride hydrate	Sigma-Aldrich	Cat# A7410
Temsirolimus	Sigma-Aldrich	Cat# PZ0020
4,7-Dimethyl-1,10-phenanthroline	Sigma-Aldrich	Cat# 301809
2-Deoxy-D-glucose	Sigma-Aldrich	Cat# D8375
Sodium dichloroacetate	Sigma-Aldrich	Cat# 347795
Dexamethasone	Sigma-Aldrich	Cat# D4902
Prostaglandin E2	Sigma-Aldrich	Cat# P0409
StemRegenin 1	Cayman Chemical	Cat# 10625

(*Continued on next page*)

Continued

REAGENT or RESOURCE	SOURCE	IDENTIFIER
FICZ, 6-formylindolo[3,2-b]carbazole	Cayman Chemical	Cat# 19529
Rotenone	Sigma-Aldrich	Cat# R8875
Critical Commercial Assays		
Enzymatic Glycemia	Wiener Lab (Argentina)	Cat# 1400060
Lactate	Wiener Lab (Argentina)	Cat# 1999795
Human IL-1β ELISA Set II	BD Biosciences	Cat# 557953
Human IL-6 ELISA Set	BD Biosciences	Cat# 555220
Human IL-8 ELISA Set	BD Biosciences	Cat# 555244
Human IL-10 ELISA Set	BD Biosciences	Cat# 555157
Human IL-12 (p70) ELISA Set	BD Biosciences	Cat# 555183
Human TNF ELISA Set	BD Biosciences	Cat# 555212
Human IL-23 DuoSet ELISA	R & D Systems	Cat# DY1290
CBA Human Th1/Th2 Cytokine Kit II	BD Biosciences	Cat# 551809
SMART-Seq v4 Ultra Low Input RNA Kit for Sequencing	Takara	Cat# 634888
RNeasy Plus Mini Kit	QIAGEN	Cat# 74136
Deposited Data		
RNA-seq Data	GEO	GSE143170
Software and Algorithms		
iDEP.90 software	Ge et al., 2018	http://bioinformatics.sdstate.edu/idep/
DESeq2	Love et al., 2014	https://bioconductor.org/packages/release/bioc/html/DESeq2.html
ShinyGO v0.61	Ge et al., 2019	http://bioinformatics.sdstate.edu/go/
tximport	Soneson et al., 2015	https://bioconductor.org/packages/release/bioc/html/tximport.html
FastQC	Andrews, 2010	https://www.bioinformatics.babraham.ac.uk/projects/fastqc/
Salmon	Patro et al., 2017	https://salmon.readthedocs.io/en/latest/salmon.html
Morpheus		https://software.broadinstitute.org/morpheus
DEBrowser	Kucukural et al., 2019	https://bioconductor.org/packages/release/bioc/html/debrowser.html
FlowJo V10	FlowJo LLC	https://www.flowjo.com
ImageJ	Schneider et al., 2012	https://imagej.nih.gov/ij/

RESOURCE AVAILABILITY

Lead Contact

Further information and requests for resources and reagents should be directed to and will be fulfilled by the Lead Contact, Jorge Geffner PhD, jorgegeffner@gmail.com.

Materials Availability

This study did not generate new unique reagents.

Data and Code Availability

The accession number for the RNA-seq data reported in this paper is GEO: GSE143170.

EXPERIMENTAL MODEL AND SUBJECT DETAILS

Human blood samples

Buffy coats from healthy donors (both male and female donors) were obtained from Sanatorio Mendez (Buenos Aires, Argentina) and heparinized human blood samples were obtained from Hospital de Clínicas "José de San Martín," Facultad de Medicina,

Universidad de Buenos Aires. All the human blood samples used in this study would have been obtained even if this study was not carried out, and they were supplied without any personal identifiable information.

METHOD DETAILS

Cell Isolation

PBMCs were isolated by centrifugation on Ficoll-Paque (GE Healthcare, Argentina). Monocytes were isolated from PBMCs by Percoll gradient centrifugation as described (Menck et al., 2014) or by positive selection using anti-CD14-coated magnetic beads according to the manufacturer's instructions (Miltenyi) (% purity 80-97). CD4+ T cells were isolated from heparinized blood samples by negative selection using RosetteSep immunodensity procedure (Cell Signaling Technologies) (% purity > 95).

Cell cultures

All the experiments were performed using RPMI-1640 medium supplemented with 50 U/ml penicillin, 50 μg/ml streptomycin and different percentages of fetal calf serum (FCS, GIBCO Invitrogen). Monocytes ($5x10^5$cells/ml) were cultured with or without the addition of M-CSF, TNFα, GM-CSF and/or IL-4 (Miltenyi) for different periods of time. L-Phytohemagglutinin (L-PHA, 1μg/ml, SIGMA/Merk) was used to stimulate PBMCs. Cultures performed in serum-free medium were performed in culture medium supplemented, or not, with 0.1% bovine serum albumin (BSA) (DSF Labs, Argentina). pH in the cultures was adjusted using isotonic HCl, as previously described (Jancic et al., 2012). pH values were determined on each day of the culture, in experiments performed in duplicate. Cultures performed at pH 7.3 remained in the pH range 7.4 to 7.2 along the culture period. Those performed at pH 6.5 remained at pH 6.5-6.8 along the culture.

Flow cytometry & cell sorting

The analysis was performed by using a BD FACSCanto cytometer and BD FACSDiva software. APC anti-CD1a (# 559775), FITC anti-CD1a (#555806), BV421 anti-CD14 (#563743), FITC anti-CD14 (#555397), PE anti-CD14 (555398), PE anti-CD16 (#347617), FITC anti-CD64 (#555527), APC anti-CD209 (#551545), PE anti-CD1c (#564900), PE anti-CD86 (# 555658), FITC anti-CD80 (#560926), FITC anti-HLA-DR (#555811), APCCy7 anti-HLA-DR (#335796), APCCy7 anti-CD11b (#557754), APC anti-CD11c (#559877) were obtained from BD Biosciences. Sorting of $CD1a^+CD16^-$ cells was performed using a BD FACSCanto cytometer.

Fluorescence and confocal microscopy

Cells were washed with PBS and resuspended in fresh RPMI medium followed by 30 minutes adhesion on poly-L-Lysine coated glass coverslips. Attached cells were washed with PBS and fixed with 4% PFA solution at 4° for 15 min. Afterward, coverslips were treated for 10 minutes with glycin 0.1M in PBS solution to quench aldehyde group autofluorescence and blocked with 1% BSA solution in PBS. Coverslips were then incubated for 1h at room temperature with mouse IgG anti-human-CD1a (#555805) in PBS 1% BSA (1:50 dilution) washed and incubated for 1h at room temperature with Alexa488 anti-mouse IgG (1:500) (Jackson Immuno Research) and Alexa594-phalloidin (Thermo Fisher) (1:200). The coverslips mounted with DAPI-Fluoromount-G (Southern-Biotech) were examined under a confocal microscope (ZEISS LSM 900) using a Plan Apochromat 63 × 1.42 NA oil immersion objective or under an Eclipse Ti-S fluorescence microscope (Nikon) using a Plan Apochromat 100 × 1.42 NA oil immersion objective.

Measurement of cytokines by ELISA

Supernatants from monocyte-derived cells ($5x10^5$/ml), stimulated or not with LPS for 18h, were harvested and analyzed for the presence of IL-12(p70), IL-10, IL-1β, IL-23, TNFα, and IL-6. Supernatants collected from the MLRs at day 6 of culture were analyzed for the presence of IFNγ, IL-5, and IL-17. ELISA was performed with BD OptEIA sets according to the manufacturer recommendations or using CBA Human Th1/Th2 Cytokine Kit II (BD).

Mixed Lymphocyte Reaction

Isolated CD4+ T cells (1×10^7 cells/ml) were labeled with 5 μM CFSE (Molecular Probes, Invitrogen) in PBS for 5 min at 37 °C. Cells were washed and plated ($2x10^5$/200 μl) in 96 well plates. Allogeneic monocyte-derived cells were counted and added to lymphocytes using an APC/CD4+T cell ratio of 1:10, 1:4 or 1:2. After 6 days of culture, cells were harvested and CFSE dilution was assessed by flow cytometry. Quantification of CD4+ T cell proliferation was determined by determining the fraction of T cells that diluted CFSE dye.

Measurement of intracellular pH

It was performed using BCECF-AM as previously described (Chow et al., 1996). Briefly, monocytes ($1x10^6$/ml) were loaded in PBS with 1 μg/ml BCECF-AM during 15 min at 37 °C, washed in PBS, and resuspended in culture medium (5×10^5/ml), adjusted to different pH values, in the absence or presence of the Na^+/H+ antiporter inhibitor amiloride (100nM). Then, cells were cultured for 12 h in the presence of M-CSF + TNFα + IL-4 and the values of intracellular pH for each condition were determined. The analysis was performed by flow cytometry, with excitation at 488 nm and emission analysis at FL1 and FL3. The intracellular pH was

calculated from the ratio of emission intensities at the two wavelengths, standardizing by comparison with the fluorescence intensity ratios of cells whose pHi values were fixed by incubation with nigericin (10 μM) in high-potassium buffers.

Analysis of glucose and lactate concentrations

Monocytes were cultured under different conditions at a concentration of $5x10^5$ cells/ml. After 3 days, glucose and lactate concentrations in culture supernatants were assessed using conventional enzymatic methods according to the manufacturer's recommendations: Enzymatic Glycemia (#1400060) and Lactate (#1999795) determination kits from Wiener Lab, Argentina.

Cell lysates and immunoblots

Cells were washed in cold PBS and pellets were lysed in 4 x Laemmli sample buffer (Bio-Rad) with the addition of phosphatase inhibitor (Merk) and protease inhibitor cocktails (Roche). Equal amounts of lysates were separated on 12% SDS-PAGE, blotted on Polyvinylidene Fluoride Transfer Membrane (Thermo Fisher Scientific). Blots were revealed using SuperSignal West Pico Chemiluminescent Substrate (Thermo Fisher Scientific). The intensity of the bands was quantified using the software ImageJ (National Institutes of Health) (Schneider et al., 2012). Anti Phospho-p70 S6 Kinase (Thr389) antibody (#9205, Cell Signaling) and Anti β-actin (#MA5-15739, Thermo Fisher Scientific- Invitrogen) were used as primary antibodies. HRP conjugated secondary antibodies were purchased from Jackson ImmunoResearch.

RNA-seq library preparation

RNA from sorted cells (250.000-500.000 $CD1a^+CD16^-$ cells) was extracted by using RNeasy Mini Kit (QIAGEN), including on-column DNase digestion as described by the manufacturer's protocol. The integrity of the RNA was confirmed in BioAnalyzer using RNA 6000 Pico kit (Agilent Technologies). cDNA was generated with SMART-Seq v4 Ultra Low Imput RNA Kit for Sequencing (Takara) following manufacturer instructions. In order to amplify the RNA, 14 cycles were used. The quantity and quality of cDNA were assessed with Qubit dsDNA high sensitivity (Thermofisher) and an Agilent Bioanalyzer using nanochip (Agilent Technologies), respectively. Unique dual indexed libraries were obtained using Kapa HyperPlus Kit (Roche) based on cDNA as starting materials. Sequencing of a pool of multiplexes libraries was performed on a NovaSeq system (Illumina) using a S1 flow cell in a paired-end 100 nts mode (PE100) allowing to get an minimum average depth of 20 million reads. Libraries, sequencing and quality control of the sequencing were performed by the ICGex NGS facility at Institut Curie.

RNA-seq analysis

Genome assembly was based on the Genome Reference Consortium (hg38). Quality of RNA-seq data was assessed using FastQC (Andrews, 2010). Reads were pseudo-aligned to the transcriptome using Salmon (Patro et al., 2017) and transcript expression values were summarized using tximport (Soneson et al., 2015). Identification of the top 500 highly variable was performed using iDEP.90 software (http://bioinformatics.sdstate.edu/idep/) (Ge et al., 2018). Genes with < 1 CPM in at least 3 libraries were filtered out, and counts data was transformed for clustering and PCA using EdgeR (log2(CPM+c)) (pseudocount c = 4). Unsupervised K means clustering of the 500 highly variable genes was performed considering 3 clusters and mean centered gene normalization. Differential gene expression analysis was performed using iDEP.90 software (Ge et al., 2018) and the Bioconductor package DESeq2 (Love et al., 2014). Statistically significant differentially expressed genes were considered when < 0.05 FDR and FC > 1. The list of upregulated and downregulated differentially expressed genes was used for pathway analysis using ShinyGO v0.61 (Ge et al., 2019) (http://bioinformatics.sdstate.edu/go/) and the databases: Reactome, KEGG and GO Biological process. Heatmaps were plotted using Morpheus (https://software.broadinstitute.org/morpheus). Volcano plots were performed using R Studio Version 1.2.5001 and DE-Browser shinny application (Kucukural et al., 2019).

Chemicals

Amiloride hydrochloride hydrate, temsirolimus, 4,7-dimethyl-1,10-phenanthroline, 2-deoxyglucose (2DG), dichloroacetate (DCA), dexamethasone, and PGE2 were purchased from Sigma-Aldrich-Merck. Stemregenin 1 and 6-formylindolo[3,2-b]carbazole (FICZ) were purchased from Cayman Chemical Company.

QUANTIFICATION AND STATISTICAL ANALYSIS

Statistical analysis

Data were analyzed using Wilcoxon nonparametric paired test in which P values of < 0.05 were considered statistically significant. Analysis was performed using GraphPad Prism V5. "n" corresponds to the number of individual donors analyzed.